Iranian Journal of Hydrogen & Fuel Cell 1(2022) 27-38

Iranian Journal of HYDROGEN FUEL & CELL

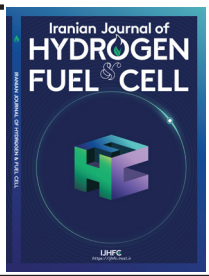

Performance verification of a laboratory scale hydrogen/oxygen combustion chamber

Ali Saberimoghaddam[a,*], Elahe Basafa[a]

[a] Faculty of Chemistry and Chemical Engineering, Malek-Ashtar University of Technology

Article Information

Article History:

Received:
28 Oct 2021
Received in revised form:
24 Dec 2021
Accepted:
9 Jan 2022

Keywords

Hydrogen/Oxygen Engine
Performance
Specific Impulse
Characteristic Velocity

Abstract

Liquid propellant missiles are commonly applied to launch satellites that must be located in upper orbits. These systems normally use hydrogen and oxygen propellants that are non-hypergolic mixtures. In this study, the test results of a designed hydrogen/oxygen engine were evaluated, and a designed spark igniter was successfully used to start the engine. Seven hot tests were carried out to determine the performance of the engine. The effect of oxygen to fuel ratio (O/F ratio) at a constant combustion chamber pressure (800 kPa) showed that the maximum value of the specific impulse (Isp) and characteristic velocity (C*) occurs at an O/F ratio of about 2.8. Experimental tests at the constant O/F ratio of 2.8 showed that performance parameters, such as Isp and C*, were enhanced when the chamber pressure was increased. However, the trend was sluggish at pressures higher than 800 kPa.

1. Introduction

Rocket propulsion has an important role in space travel and launching satellites/payloads into the orbits around the earth. A chemical rocket consists of an injector, a combustion chamber, and a nozzle. The high-pressure combustion gases expand and reach a high velocity through the converging-diverging nozzle. At the throat of the nozzle the gases' velocity reaches the local speed of sound, and their velocity becomes supersonic at the nozzle outlet[1,2].

Several fields should be considered to design and test

*Corresponding Author:

doi: 10.22104/IJHFC.2021.5273.1232

a rocket engine, such as electrical engineering, thermal concepts, structural dynamics, and fluid dynamics. Additionally, a good consistency between analytical and physical interfaces is needed to develop an acceptable propulsion system[3]. A liquid rocket engine is a sophisticated system with lots of parts, including fuel/oxidizer injection elements, a combustion chamber, pipelines, valves, etc., which must intercommunicate with each other[4].

The type of propellant employed in the rocket engine is also important. Green propellants that produce lower poisonous and cancerous gases in the nozzle exhaust are known as environmentally friendly propellants, and they have received a lot of attention in the last decades[5]. These hydrogen/oxygen systems are fascinating subjects in the rocket industry because of specific characterizations like a simple combustion system with elementary reactions, high chemical energy capacity, non-toxicity of the produced gases, availability, and high specific impulse[6-9]. Due to its high enthalpy of combustion (40 kWh/kg) compared to hydrocarbon fuels (about 12 kWh/kg), hydrogen is an economical, environmentally friendly fuel with desirable performance[10-12].

As mentioned, the rocket engine consists of several parts. One of the main parts is the feed system, which is required to inject the propellants into the thrust chamber with a specific pressure and flow rate. A pressure-fed system is not as complicated as others. This system is suitable for low quantities of propellants with low pressure and consists of pressurized tanks, a regulator, valves, feed lines, flow controllers, pressure transmitters, and a thrust chamber. Despite the high weight of the pressurized tanks, a pressure-fed system has diverse advantages like low cost and simplicity due to its few constituent parts[13,14].

It can be claimed that the thrust chamber is the most important part of the engine. The propellants are injected and atomized through an igniter in the thrust chamber, where they are mixed, burned, and attain a temperature above 3500 K. Ultimately, the produced combustion gases expand to supersonic velocities in the nozzle[15,16]. The thrust achieved by ejection of the expanded gases resulting from the burned propellants is generated based on Newton's third law of motion[1].

An important part of the thrust chamber is the igniter. Hydrogen/oxygen is a non-hypergolic propellant. This means that a reliable ignition system is needed to ignite the gases in the combustion chamber. Therefore, studies on ignition systems have been of constant interest[17,18]. An electrical spark igniter with lower required power and least mass and volume would be more desirable[19-22]. Also, high energy sparks with a short duration are required for assured ignition of flammable propellants[22]. Propellants must pass through the injector to enter the combustion chamber. The most common injector employed in the hydrogen/oxygen system is the coaxial type. The main engines of the space shuttles and the RL-10 engines of Atlas Centaur use coaxial straight-flow injectors[23-28].

Many parameters, such as fabrication process and assembly quality, production cost, firing test, and performance validation, should be considered in the manufacture of the rocket engine. The test of subsystems, such as the igniter, thrust chambers, and combustion chamber, is an important elemental step to develop and prepare the whole rocket engine system[29-31]. Consequently, the performance accuracy of different parts of the engine should be examined before the hot test. All equipment, such as pressure transmitters, temperature transmitters, flow controllers, solenoid valves, and also some parts of the thrust chamber, like the igniter, injector, and load cell, must be checked before testing the entire system. All feed lines and engine parts should be purged with inert gases like nitrogen to ensure the lack of leakage and contamination. The targets of the engine hot-fire test are: 1- confirmation of the true assembly and fabrication of the engine, 2- identification of any defective parts, 3- calibration of the engine control variables, and 4- confirmation of the engine performance (thrust and specific impulse). After the tests, the resulting data should be analyzed and compared with the predictive model[32-35]. Owing to common defects in the mixing, combustion, and expansion of the propellants, operational results are often different from the calculated theoretical results[36].

The hydrogen/oxygen rocket engine has been investigated in previous research. Twardy[37] studied gaseous hydrogen/oxygen propellants in a variable-thrust rocket engine at a constant combustion chamber pressure of 200 kPa and maximum nominal thrust of 8000 N. The effects of variation of the mixture ratio and throttling on combustion chamber efficiency were also studied, and the use of a modified expansion-deflection-nozzle was offered for better performance. Sternfeld et al.[38] studied the LOX/GH_2 high-pressure rocket engine at a combustion chamber pressure of 30 MPa and propellant mass flow rate of 9.5 kg/s. To assess the flow and combustion specifications, a complex laser-based diagnostic was employed in this study for non-intrusive

measurement. Kirner, Thielemann, and Wolf[39] studied the application of cryogenic propellants LOX/LH_2 at a chamber pressure of 10^4 kPa in a Vulcain engine and achieved a vacuum specific impulse of 439 s. Chiaverini et al.[40] reported the variations of specific impulse and thermal behavior of the thrust chamber influenced by the geometry of the combustion chamber, injector, and nozzle of the gaseous oxygen/hydrogen rocket. They found that if the ratio of length to diameter of the combustion chamber was more than 2, the specific impulse would be decreased. Also, narrower combustion chambers and larger fuel jets cause lower heating rates. Yanagawa et al.[41] confirmed the development of a LE-5 engine fed by LOX/LH2. A successful engine start was achieved at the combustion chamber pressure of 3600 kPa, a mixture ratio of 5.5, and a vacuum specific impulse of 448 s. Haberbusch et al.[42] showed the effect of densified LOX/LH2 on the rocket performance. The investigation of an RL10 engine revealed that colder inlet propellants enhance the thrust up to 12%, decrease the turbine/pump speeds, and reduce the pressure drop. So, the use of the densified propellants influences the payload capability and mission efficiency. Elam[43] examined the calorimeter chamber and swirl coaxial injector of aLOX/GH2 subscale rocket. It was concluded that the effects of chamber pressure variation from 1.02×10^4 to 1.16×10^4 kPa and the mixture ratio changing from 5.24 to 6.90 on the axial heating rate and wall temperature were reasonable. In addition, the use of a swirl coaxial injector resulted in satisfactory performance. Kayama et al.[44] studied the cryogenic LOX/LH2 propulsion unit with both a pressure-fed system and a pump-fed system. They reported that the pump-fed system resulted in higher I_{sp}; but, when higher reliability with a shorter development payload time is needed, the pressure-fed system is a better choice. Also, the pressure-fed system required lower costs and had lower operational risk.

In this study, a lab-scale gaseous hydrogen/oxygen rocket engine was investigated. Some parts of the studies on the rocket motor engines are related to the gaseous hydrogen/oxygen propellant. This mode is not widely used in flying rocket motors. However, due to the simplicity of the gaseous state compared to the sophisticated phenomena (like atomization and evaporation) that exist in the liquid state of hydrogen/oxygen propellants, it could be used as a preliminary step to validate the CFD simulations data[45-49]. In this study, the influence of variation of chamber pressure and mixture ratio on the rocket engine performance was investigated. Combustion chamber performance is demonstrated by the characteristic velocity defined as the effective energy level of the propellants, the design quality of the injector and combustion chamber, and also the specific impulse, which is the basic measure of a rocket engine performance[14,50,51]. Afterward, the experimental results are compared with the theoretical results obtained from the ideal rocket relations.

2. Experimental Setup

2.1. Motor Configuration

The hydrogen/oxygen thrust chamber consists of several sections, including a coaxial injector assembly, an electrical spark igniter, a convergent-divergent nozzle, and a water-cooled jacket. The thrust chamber developed in the present study was made of stainlesssteel 310. Details concerning the thrust chamber dimensions are summarized in Table 1.

Table 1. Thrust chamber specifications.

Parameter	Size
Throat diameter (D_t)	12 mm
Expansion ratio (ε_e)	6
Nozzle exhaust diameter (D_e)	25.3 mm
Combustion chamber diameter (D_c)	29.5 mm
Combustion chamber length (L_c)	96.2 mm
Nozzle convergence length ($L_{con.}$)	18.3 mm
Nozzle divergence length ($L_{div.}$)	25 mm
Nozzle convergence angle	28º
Nozzle divergence angle	15º

The used coaxial injector has a GO_2 post inner diameter of 6 mm and is not recessed. The injector's GH_2 annulus has an inner diameter of 10 mm. The combustion chamber and nozzle are cooled using a cold water jacket. A CBT310 pump with a nominal power of 2.2 kW from Pentax Italian Company was used for circulating water around the thrust chamber. Also, PT100 temperature thermometers were employed to measure the input and output water temperatures. The flow rate

of the cooling water was fixed at 635 g/s. The sizes of all pipes and fittings in this system were 1.25 inches. A pressure transmitter with a nominal measurement range of 0-5000 kPa from ALTHEN Company was used to measure the pressure of the combustion chamber in firing tests. A schematic of this lab-scale engine with details concerning the thrust chamber dimensions is shown in Fig. 1 (A). The stand used in the tests was equipped with a rocket motor supporting thrust frame, which was made moveable by a low friction linear slide for measurement of the thrust (Fig. 1 (B)). The value of the thrust was measured by a load cell with a nominal force of 2000 N from the HBM Company.

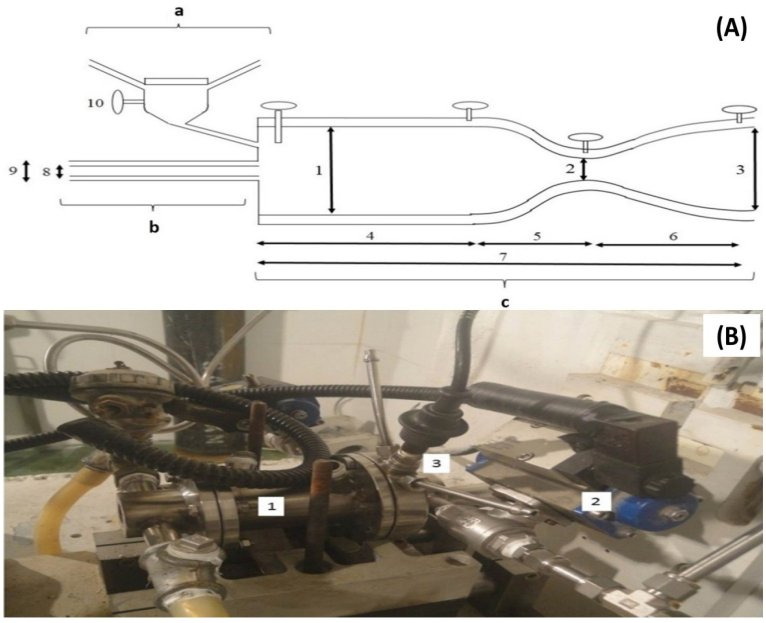

Fig. 1 (A) Gaseous H_2/O_2 rocket engine. a: Igniter, b: Coaxial injector, c: Thrust chamber, 1: Combustion chamber diameter, 2: Throat diameter, 3: Nozzle exhaust diameter, 4: Combustion chamber length, 5: Nozzle convergence length, 6: Nozzle divergence length, 7: Entire length of the thrust chamber, 8: Oxidizer inlet of injector, 9: Fuel inlet of injector, and 10: Igniter combustion chamber. (B) The test stand used for firing tests of GH2/GO2. 1: Lab-scale engine, 2: Solenoid valve of hydrogen, and 3: Igniter.

2.2. Ignition System

The gaseous hydrogen/oxygen mixture employed as the propellant for the propulsion system was non-hypergolic. Thus, an ignition system was required to provide the initial heat and energy to start the engine. A proper ignition system must be reliable, and in practice, repeatable responses should be achieved in sequential tests. An electric ignition system with hydrogen as fuel and oxygen as an oxidizer was used for firing tests. The combustion chamber of an electric-flame igniter was designed and manufactured with a throat diameter of 4.5 mm, an expansion ratio of 6, and a length of 11.8 mm. The spark system used to create the flame produces 50 sparks per second with a power of 0.4 J. The operating time of the spark system was 3 s, which could create a 10 s stable flame. The igniter was ignited with the same O/F ratio as the engine. The igniter combustion chamber specifications are summarized in Table 2. Fig. 2 (A) and (B) show the spark system and the combustion chamber of the igniter, respectively.

Table 2. Igniter specifications used for firing tests of GH_2/GO_2.

Parameter	Size (mm)
Throat diameter ($D_{t\ ign.}$)	12
Combustion chamber diameter ($D_{c\ ign.}$)	11
Combustion chamber length ($L_{c\ ign.}$)	9.9
Nozzle convergence length ($L_{con.\ ign.}$)	1.9

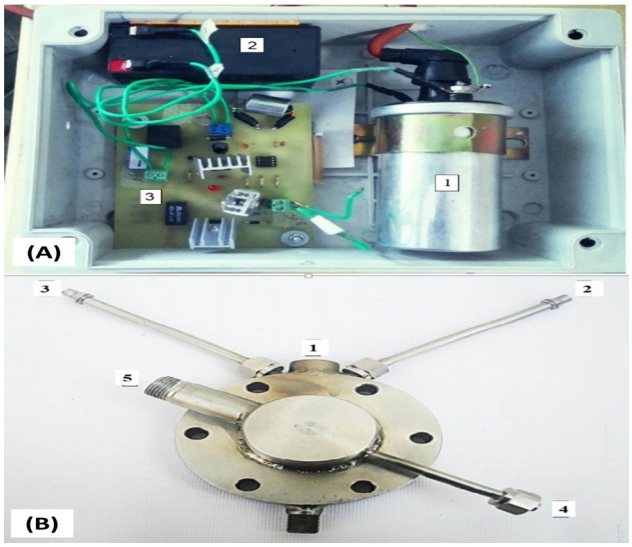

Fig. 2 (A) Spark system of the igniter. 1: Coil, 2: Battery, and 3: Electrical circuit. (B) Igniter. 1: Location of spark system, 2: Fuel inlet to the igniter, 3: Oxygen inlet to the igniter, 4: Fuel inlet to the injector of the engine, and 5: Oxygen inlet to the injector of the engine.

2.3. Instrumentation

The experimental setup is shown in Fig. 3. The feeding system is a pressure-fed type with three pressurized tanks of hydrogen, oxygen, and nitrogen. The hydrogen and oxygen gases were fuel and oxidizer gases, respectively, and the nitrogen gas was employed as the purging gas. Each tank was equipped with a regulator to adjust the outlet pressure. After passing through the needle valve, the gas reached the solenoid valve, which was controlled from the control room. The gas streams pass through the flow meters, and before entering the injector, they pass through the check valves to prevent the flow from returning to the pipeline. After each test, all hydrogen pipelines were purged by nitrogen gas.

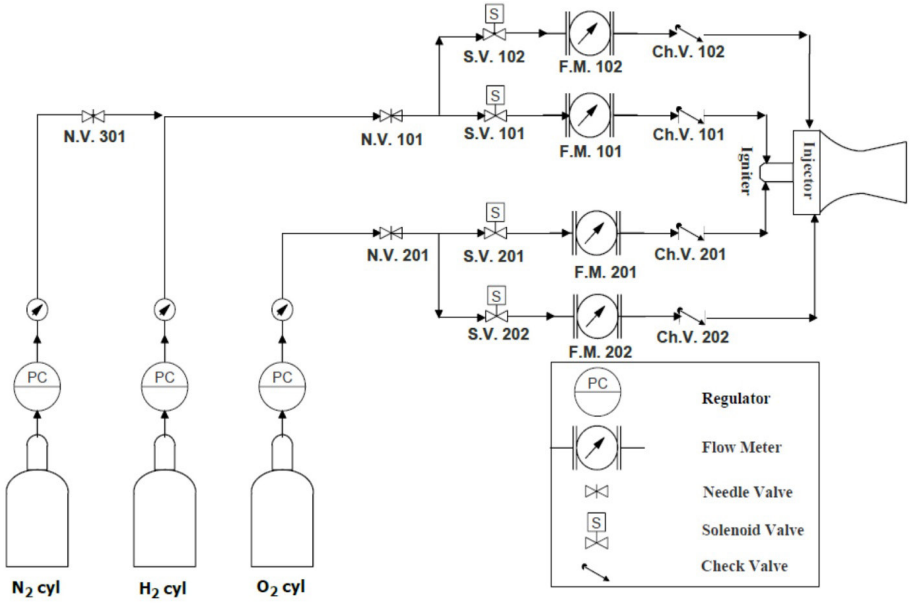

Fig. 3. Experimental setup for GH_2/GO_2 firing tests.

3. Results and Discussions

3.1. Igniter Test

To certify the reliability of the spark ignition, it should be examined separately. The rocket engine test was conducted after ensuring the accuracy of the ignition tests.

Three tests with mixing ratios of 3, 8, and 12 were performed to ensure the integrity of igniter performance at different mixing ratios. In order to study the repeatability of the igniter, ten successive combustion tests were successfully performed at a mixing ratio of

3 and a time interval of 5 s. The variations of the temperature of the thermometer on the body of the igniter as a function of the time in the repeatability test of the igniter are shown in Fig. 4.

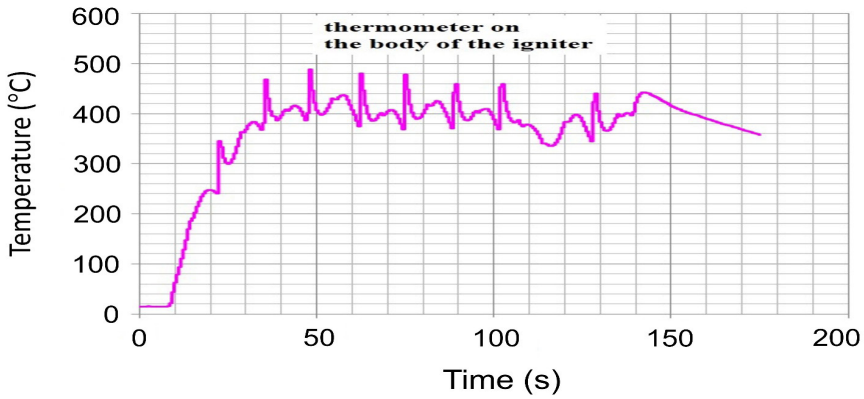

Fig. 4. Temperature of the thermometer on the body of the igniter vs. time in the repeatability test of the igniter.

3.2. Thrust Chamber Test

In this study, seven successful firing tests were accomplished. The results of the conducted tests and the technical parameters of the thrust chamber are measured, evaluated, and summarized in Table 2. The effect of variation of combustion chamber pressure on the performance parameters was considered at a constant O/F ratio (2.8) in the first three tests, while the effect of various O/F ratios on the performance parameters was studied at a constant combustion chamber pressure (800 kPa) for the rest of the tests.

The values of characteristic velocity and specific impulse listed in Table 3 were calculated by equations (1) and (2), respectively. The amounts of thrust (F) and combustion chamber pressure (P_c) were obtained from firing tests.

$$C^* = \frac{P_c . A_t}{\dot{m}} \quad (1)$$

$$I_{sp} = \frac{F}{\dot{m} . g} \quad (2)$$

Table 3. Specifications of firing tests with the lab-scale hydrogenic engine.

Test No.	Hydrogen flow rate (g/s)	Oxygen flow rate (g/s)	Total flow rate (g/s)	O/F	Combustion chamber pressure (kPa)	Thrust (N)	Specific impulse (s)	Characteristic velocity (m/s)
1	10	28	38	2.8	2900	40	121.3	890
2	13	36	49	2.8	4200	61	137.2	973.7
3	22	61	83	2.8	8700	130	155	1096.8
4	41	43	84	1.0	8200	133	149.6	1203
5	22	65	87	2.9	8100	137	158.5	1274
6	14	71	85	5.0	8000	133	150.5	1201
7	9	74	83	8.8	8200	132	129.5	1032

As a sample, Fig. 5 shows the graph of combustion chamber pressure and thrust vs. time for the test number 4 from Table 3.

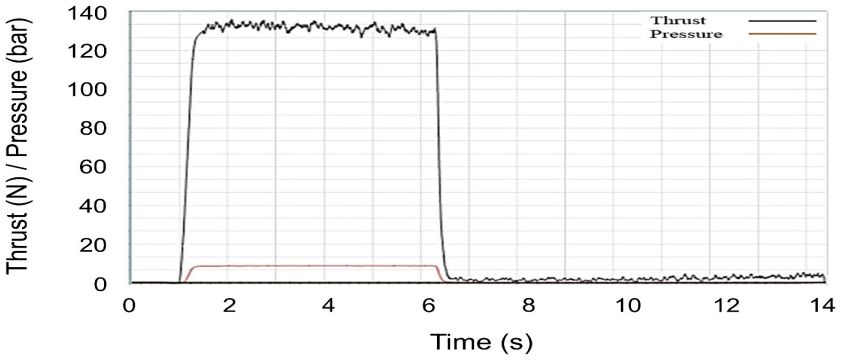

Fig. 5. Results of motor thrust and chamber pressure vs. time for test No. 4 from Table 3.

A delay time of about 1 s was observed between the start-up of the system and combustion for the firing tests of the engine. This delay time was due to the time required for the values to open and the fuel to reach the spark system, mixing the fuel with oxygen, combustion of fuel and oxidizer, and thermometer response.

To determine the performance efficiency of the hydrogenic motor, test results were compared with the corresponding theoretical values of an ideal rocket performance calculated by the relevant basic thermodynamic principles. According to the theoretical thermodynamic calculation and analysis, the ideal thrust was determined by the equation (3)[52]:

$$F = A_t P_1 \sqrt{\frac{2k^2}{k-1}} \left(\frac{2}{k+1}\right)^{(k+1)/(k-1)} \left[1-\left(\frac{P_2}{P_1}\right)^{(k-1)/k}\right] + (P_2 - P_3)A_2 \quad (3)$$

Where A_t is the throat area, A_2 is the nozzle exit area, P_1 is the combustion chamber pressure, P_2 is the nozzle exit pressure, P_3 is the atmospheric pressure, and k is the specific heat ratio. The ratio of the throat area to any downstream area could be defined as a function of the ratio of specific heats and pressure ratio. Therefore, using equation (4), the pressure ratio can be determined at any specified amount of area ratio, and vice versa[52].

$$\frac{A_t}{A_x} = \left(\frac{k+1}{2}\right)^{\frac{1}{k-1}} \left(\frac{P_x}{P_1}\right)^{\frac{1}{k}} \sqrt{\frac{k+1}{k-1}\left[1-\left(\frac{P_x}{P_1}\right)^{\frac{k-1}{k}}\right]} \quad (4)$$

The specific impulse and characteristic velocity, which are the primary performance measures for the propellant, are also calculated by equations (5) and (6), respectively[52].

$$I_{sp} = \frac{1}{g}\sqrt{\frac{2k}{k-1}\frac{RT_0}{M}\left[1-\left(\frac{P_2}{P_1}\right)^{\frac{k-1}{k}}\right]} \quad (5)$$

$$C^* = \frac{P_1 A_t}{\dot{m}} = \frac{\sqrt{kRT_0}}{k\sqrt{\left[\frac{2}{(k+1)}\right]^{(k+1)/(k-1)}}} \quad (6)$$

Where M is the average molecular weight of produced combustion gases, and T_0 is the combustion chamber temperature. Some of the parameters in these equations were calculated using the PROPEP[1] software. So, using the equations above, the ideal values of thrust, specific impulse, and characteristic velocity were calculated for the conditions mentioned in Table 2 for every test. It is clear that specific impulse is a function of the ratio of specific heats k, the pressure ratio P_1/P_2, and the ratio of the absolute nozzle entrance temperature to the molecular mass. T/M is an important factor in determining the mixture ratio of propellants. Increasing the exhaust gas temperature resulting from the increase in released energy of combustion would influence the rocket performance. Also, decreasing the molecular mass of the propellant obtained by using the low molecular mass gases would have the same effect on the rocket performance. In addition, the characteristic velocity C^* is a function of the combustion chamber design and propellant features, while it is independent of nozzle characteristics[52].

1. Propellant Equilibrium Program

The variation of thrust versus combustion chamber pressure for both the experimental firing tests and theoretical data obtained from the above equations are represented in Fig. 6(A). As could be observed, at a certain mixture ratio (2.8), the ideal thrust calculated from equation (1) varies linearly with respect to the combustion chamber pressure. So, by increasing the propellant flow rate in a constant mixture ratio, the combustion chamber pressure would be increased, and as a result, the thrust would be enhanced. Therefore, the obtained linear relationship could be employed for interpolating and determining the thrust value at any given combustion chamber pressure. As shown in Fig. 6(A), the test results are consistent with the theoretical graph.

The experimental and theoretical variations of the specific impulse as a function of the combustion chamber pressure are shown in Fig. 6(B). Fig. 6(B) shows the relationship between specific impulse and combustion chamber pressure. As can be seen, by enhancing the combustion chamber pressure, the specific impulse would be increased, which is in agreement with the test results. Furthermore, Fig. 6(B) shows that the dependency of the specific impulse to P_c at higher pressures becomes sluggish. This can be justified by the fact that at low pressures, the combustion efficiency is low, and therefore the dependency of I_{sp} to P_c is considerable. While at high pressures, the combustion is completed, and thus the dependency of I_{sp} to P_c is not high.

Fig. 6(C) shows the plot of the specific impulse vs. O/F ratio at constant combustion chamber pressure (800 kPa). As demonstrated in Fig. 6(C), the experimental and theoretical specific impulse exhibited a similar dependency on the O/F mixture ratio.

The mass flow rate ratio of oxidizer to fuel influences the engine performance by affecting the combustion chemistry, tank sizes, and weight[14].

In the hydrogen/oxygen propulsion system, the amount of mixture ratio should be determined so that the maximum specific impulse can be achieved, which results in obtaining the optimum performance[49]. Very similar results were obtained by Song et al.[7] for an optimum amount of O/F mixture ratio. They reported that the maximum amount of ideal specific impulse was revealed in the O/F range of 2 to 3, and at both higher and lower O/F values relative to the mentioned range, the specific impulse was decreased.

Characteristic velocity determines a measure of the combustion efficiency[40]. Fig. 6(D) shows the plot of characteristic velocity vs. the O/F ratio at constant combustion chamber pressure (800 kPa). This figure shows that the plot of ideal and experimental results of variations of C^* vs. O/F passes through a maximum at the O/F ratio of about 2.8 to 3. A similar dependence on mixture ratio was observed for the specific impulse in Fig. 6(C).

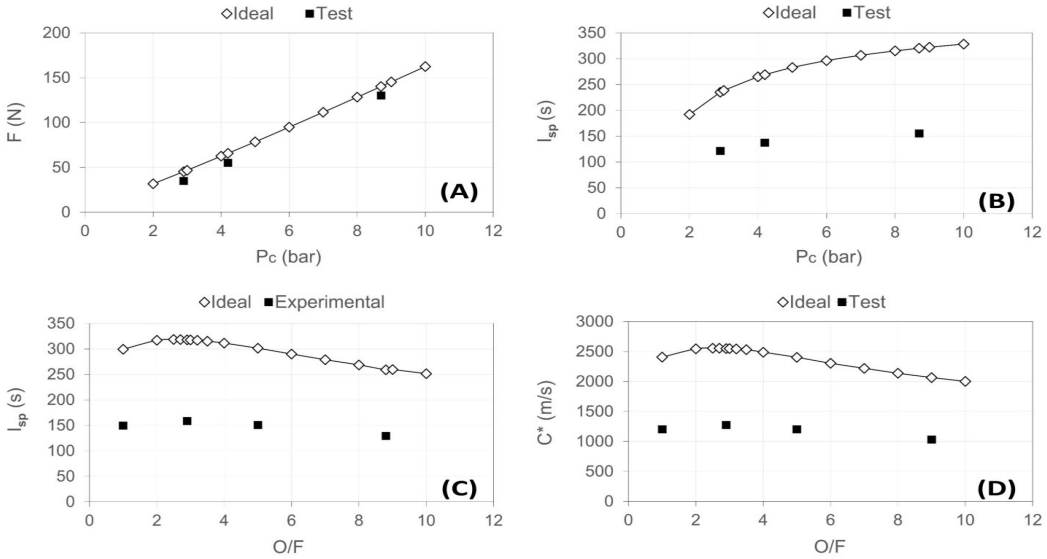

Fig. 6(A) Comparison of ideal and test thrust vs. combustion chamber pressure at a constant O/F (2.8). (B) Comparison of ideal and test specific impulse vs. combustion chamber pressure at a constant O/F (2.8). (C) Comparison of ideal and experimental specific impulse vs. O/F ratio at a constant combustion chamber pressure (800 kPa). (D) Comparison of ideal and test characteristic velocity vs. O/F ratio at a constant combustion chamber pressure (800 kPa).

4. Conclusion

A laboratory-scale experimental setup for testing a hydrogenic engine was established and successfully utilized in this study. A spark igniter was successfully used to ignite the propellants for the hydrogenic engine. Seven firing tests were conducted to examine the performance integrity of the hydrogen rocket engine. The effects of the mixture ratio and combustion chamber pressure on engine performance were investigated. The experimental tests showed that when the combustion chamber pressure is increased, the performance parameters, such as thrust, specific impulse, and characteristic velocity, are enhanced. The effect of the O/F ratio on performance parameters at a constant combustion chamber pressure showed the maximum value of these parameters occurs at an O/F ratio of about 2.8. The test results were consistent with the ideal rocket relationships.

Nomenclature

A_t	throat area (m^2)
A_2	nozzle exit area (m^2)
C^*	characteristic velocity (m/s)
F	thrust (N)
I_{sp}	specific impulse (s)
k	specific heat ratio (-)
$\dot{m}$	propellant flow rate (kg/s)
M	average molecular weight of produced combustion gases (kg/kmol)
O/F	oxygen to fuel ratio (-)
P_1	combustion chamber pressure (kPa)
P_2	nozzle exit pressure (kPa)
P_3	ambient pressure (kPa)
T_0	combustion chamber temperature (K)

Acknowledgements

The authors would like to acknowledge the support by the Malek-Ashtar University of Technology.

References

[1]. Thakre, P. Rocket propulsion: Basic concepts and introduction. *Encyclopedia Aerosp. Eng.*, John Wiley & Sons, Ltd., 2010. doi.org/10.1002/9780470686652.eae100.

[2]. Karmarkar, K. Rocket. *Def. Sci. J.*, 2013, ***2***(4), 218-221. doi.org/10.14429/dsj.2.3448 .

[3]. Emdee, J.L. Liquid propulsion: Systems engineering, design trades, and testing. *Encyclopedia Aerosp. Eng.*, John Wiley & Sons, Ltd., 2010. doi.org/10.1002/9780470686652.eae111.

[4]. Sunakawa, H.; Okita, K.; Tamura, T.; Ogawara, A.; Mitsuhashi, K.; Kobayashi, S.; Kurosu, A.; Onga, T. & Mizuno, T. Robust and optimized design for liquid rocket engine. *Am. Inst. Aeronaut. Astronaut.* , 2009, 5137. doi.org/ 10.2514/6.2009-5137.

[5]. Gohardani, A.S.; Stanojev, J.; Demairé, A.; Anflo, K.; Persson, M.; Wingborg, N. & Nilsson, C. Green space propulsion: Opportunities and prospects. *Prog. Aerosp. Sci.*, 2014, **71**, 128-149. doi.org/10.1016/j.paerosci.2014.08.001.

[6]. Maas, U. & Warnatz, J. Ignition processes in hydrogen-oxygen mixtures. *Combust. Flame*, 1988, **74**(1), 53-69. doi.org/10.1016/0010-2180(88)90086-7.

[7]. Song, Y.; Yu, N.; Zhang, G.; Ma, B.; Zhou, W. & Huang, X. Investigation of novel hydrogen/ oxygen thruster for orbital maneuver in space station. *Chinese J. Aeronaut.*, 2005, **18**(4), 289-294. doi.org/10.1016/S1000-9361(11)60247-1.

[8]. Robinson, J.W.; Rhodes, R.E. & Henderson, E.M. Mostly-reusable LOX/H2 space transportation concept enabled through advanced technologies. *Am. Inst. Aeronaut. Astronaut.*, 2014, 3650. doi.org/10.2514/6.2014-3650.

[9]. Surmacz, P. Green rocket propulsion research and development at the institute of aviation: problems and perspectives. . *int j. hydrogen energy,* 2016, **42**(39). doi.org/10.5604/12314005.1213534

[10]. Lidor, A.; Weihs, D. & Sher, E. Theoretical analysis of the explosion limits of hydrogen-oxygen system. *Am. Inst. Aeronaut. Astronaut.*, 2017, 0839. doi.org/10.2514/6.2017-0839.

[11]. Cecere, D.; Giacomazzi, E. & Ingenito, A. A review on hydrogen industrial aerospace applications. *int j. hydrogen energy*, 2014, **39**(20). doi.org/10.1016/j.ijhydene.2014.04.126.

[12]. Petrescu, R.V.V.; Machín, A.; Fontánezc, K.; Arango, J.C.; Márquezc, F.M. & Petrescua, l. I.T. Hydrogen for aircraft power and propulsion**.** *int j. hydrogen energy,* 2020, 45(41). doi.org/10.1016/j.ijhydene.2020.05.253.

[13]. Cannon, J.L. Liquid propulsion: Propellant feed system design. *Encyclopedia Aerosp. Eng.*, John Wiley & Sons, Ltd., 2010. doi.org/10.1002/9780470686652.eae110.

[14]. Kim, E. S.; Emdee, J.L. & Cohn, R.K. Liquid propulsion: Historical overview, fundamentals, and classifications of liquid rocket engines. *Encyclopedia Aerosp. Eng.*, John Wiley & Sons, Ltd., 2010. doi.org/10.1002/9780470686652.eae107.

[15]. Cai, G.; Fang, J.; Xu, X. & Liu, M. Performance prediction and optimization for liquid rocket engine nozzle. *Aerosp. Sci. Technol.*, 2007, **11**(2-3), 155-162. doi.org/10.1016/j.ast.2006.07.002.

[16]. Frey, M.; Aichner, T.; Görgen, J.; Ivancic, B.; Kniesner, B. & Knab, O. Modeling of rocket combustion devices. *Am. Inst. Aeronaut. Astronaut.*, 2010, 4329. doi.org/10.2514/6.2010-4329.

[17]. Börner, M.; Manfletti, C.; Hardi, J.; Suslov, D.; Oschwald, M. & Kroupa, G. Comparison of laser ignition and torch ignition in a subscale rocket combustor. *Am. Inst. Aeronaut. Astronaut.*, 2018, 4946. doi.org/10.2514/6.2018-4946.

[18]. Armbruster, W.; Hardi, J.S.; Suslov, D.; Oschwald, M. Injector-driven flame dynamics in a high-pressure multi-element oxygen-hydrogen rocket thrust chamber, *Journal of propulsion and power*, 2019, 35(3). doi.org/10.2514/1.B37406.

[19]. Thompson, B.F.; Strack, D.F. & Mungas, G. Determining electrical ignition characteristics of a gas propulsion system. *J. Spacecraft Rockets*, 2016, **53**(5). doi.org/10.2514/1.A33468.

[20]. Brieschenk, S.; Pontalier, Q.; Duffaut, A.; Denman, Z.J.; Veeraragavan, A.; Wheatley, V. & Smart, M. Characterization of a spark ignition system for flameholding cavities. *Am. Inst. Aeronaut. Astronaut.*, 2014, 2242. doi.org/10.2514/6.2014-2242.

[21]. Whitmore, S.A.; Inkley, N.R.; Merkley, D.P. & Judson, M.I. Development of a power-efficient, restart-capable arc igniter for hybrid rockets. *J. Propul. Pow.*, 2015, **31**(6), 1739. doi.org/10.2514/1.B35595.

[22]. Kim, J.; Sforzo, B.; Seitzman, J. & Jagoda, J. High energy spark discharges for ignition. *Am. Inst. Aeronaut. Astronaut.*, 2012, 4172. doi.org/10.2514/6.2012-4172.

[23]. Gill, G.S. & Nurick, W.H., Liquid rocket engine injectors, NASA-SP-8089, NASA Lewis Research Center, Cleveland, OH, USA, 1976.

[24]. Mayer, W.; Schik, A.; Schaffler, M. & Tamura, H. Injection and mixing processes in high-pressure liquid oxygen/gaseous hydrogen rocket combustors. *J. Propul. Pow.*, 2000, **16**(5), 823-828. doi.org/10.2514/2.5647.

[25]. Yang, V.; Habiballah, M.; Hulka, J. & Popp, M., Liquid rocket thrust chambers: Aspects of modeling, analysis, and design, *Am. Inst. Aeronaut. Astronaut.*, Inc., Virginia, 2004.

[26]. Mayer, W. & Tamura, H. Propellant injection in a liquid oxygen/gaseous hydrogen rocket engine. *J. Propul. Pow.*, 1996, **12**(6), 1137-1147. doi.org/10.2514/3.24154.

[27]. Mayer, W.O.H.; Schik, A.H.A; Vielle, B.; Chauveau, C.; Gokalp, I.; Talley, D.G. & Woodward, R.D. Atomization and breakup of cryogenic propellants under high pressure subcritical and supercritical conditions. *J. Propul. Pow.*, 1998, **14**(5), 835-842. doi.org/10.2514/2.5348.

[28]. Mayer, W.O.H. Coaxial atomization of a round

liquid jet in a high speed gas stream: A phenomenological study. *Exp. Fluids*, 1994, **16**, 401-410. doi.org/10.1007/BF00202065.

[29]. Langel, G.; Mattstedt, T.; Luger, P. & Ziegenhagen, S. Test verification of the cryogenic Vinci thrust chamber. *Am. Inst. Aeronaut. Astronaut.*, 2006, 4903. doi.org/10.2514/6.2006-4903.

[30]. Kumar, A. & Anjaneyulu, L. Emerging trends in instrumentation in rocket motor testing. *Def. Sci. J.*, 2015.,*65*(1), 63-69. doi.org/10.14429/dsj.65.7949.

[31]. Venugopal, S.; Ramanujachari, V. & Rajesh, K. Design and testing of lab-scale red fuming nitric acid/hydroxyl-terminated polybutadiene hybrid rocket motor for studying regression rate. *Def. Sci. J.*, 2011, *61*(6), 515-522. doi.org/10.14429/dsj.61.873.

[32]. Leahy, J.C.; Hanna S.G.; Malchi, J.Y. & Kim, E.S. Liquid propulsion: Engine production and operation. *Encyclopedia Aerosp. Eng.*, John Wiley & Sons, Ltd., 2010. doi.org/10.1002/9780470686652.eae112.

[33]. Krishnamachary, S.; Mohan, S.; Kulkarni, S. G.; Jayaraman, D.; Rao, M.; Singh, L. & Prasad, S. Propellant grade hydrazine in mono/bi-propellant thrusters: preparation and performance evaluation. *Def. Sci. J.*, 2015, *65*(1), 31-38. doi.org/10.14429/dsj.65.7986.

[34]. Galeev, A.G. Review of engineering solutions applicable in tests of liquid rocket engines and propulsion systems employing hydrogen as a fuel and relevant safety assurance aspects**,** *int j. hydrogen energy,*2017, 42(39). doi.org/10.1016/j.ijhydene.2017.06.242.

[35]. Rodchenko, V.V.; Galeev, A.G.; Popov, B.B. & Galeev, A.V. Study of security systems of oxygen-hydrogen propulsion plant test on the stand, *alternative energy and ecology,*2015. doi.org/10.15518/isjaee.2015.20.005.

[36]. Hagemann, G.; Immich. H.; Nguyen., T.V. & Dumnov, G.E. Advanced rocket nozzles. *J. Propul. Pow.*, 1998, **14**(5). 620-634. doi.org/10.2514/2.5354.

[37]. Twardy, H. On a variable-thrust hydrogen-oxygen rocket engine. *Acta Astronaut.*, 1975, **2**(7-8), 627-647. doi.org/10.1016/0094.5765(75)90006-5.

[38]. Sternfeld, H.J.; Haidn, O.J.; Potier, B.; Vuillermoz, P. & Popp, M. International cooperation on hydrogen/oxygen high pressure combustion. *Acta Astronaut.*, 1995, **37**, 487-496. doi.org/10.1016/0094-5765(95)00075-B.

[39]. Kirner, E.; Thelemann, D. & Wolf, D. Development status of the Vulcain thrust chamber. *Acta Astronaut.*, 1993, **29**(4), 271-282. doi.org/10.1016/0094-5765(93)90140-R.

[40]. Chiaverini, M.J.; Malecki, M.J.; Sauer, J.A.; Knuth, W.H.; Gramer, D.J. & Majdalani, J. Vortex thrust chamber testing and analysis for O2/H2 propulsion applications. *Am. Inst. Aeronaut. Astronaut.*, 2003, 4473. doi.org/10.2514/6.2003-4473.

[41]. Yanagawa, K.; Fujitat, T.; Miyajima, H. & Kishimoto, K. High-altitude simulation tests of the LOX/LH2 engine LE-5. *J. Propul. Pow.*, 1985, **1**(3), 180-186. doi.org/10.2514/3.22779.

[42]. Haberbusch, M.S.; Nguyen, C.T.; Skaff, A.F. & Lobo, S. Modeling RL10 thrust increase with densified LH2 and LOX propellants. *Am. Inst. Aeronaut. Astronaut.*, 2003, 4485. doi.org/10.2514/6.2003-4485.

[43]. Elam, S.K. Subscale LOX/hydrogen testing with a modular chamber and a swirl coaxial injector. *Am. Inst. Aeronaut. Astronaut.*, 1991, 1874. doi.org/10.2514/6.1991-1874.

[44]. Kayama, A.; Watanabe, A.; Shibato, Y. & Godai, T. Small cryogenic propulsion unit for upper stage application. *Acta Astronaut.*, 1985, **12**(3), 163-170. doi.org/10.1016/0094-5765(85)90057-8.

[45]. Marshall, W.; Pal, S.; Woodward, R. & Santoro, R. Benchmark wall heat flux data for a GO2/GH2 single element combustor. *Am. Inst. Aeronaut. Astronaut.*, 2005, 3572. doi.org/10.2514/6.2005-3572.

[46]. Tucker, P.K.; Menon, S.; Merkle, C.L.; Oefelein, J.C. & Yang, V. Validation of high-fidelity CFD simulations for rocket injector design.

Am. Inst. Aeronaut. Astronaut., 2008, 5226. doi.org/10.2514/6.2008-5226.

[47]. Sozer, E.; Vaidyanathan, A.; Segal, C. & Shyy, W. Computational assessment of gaseous reacting flows in single element injector. *Am. Inst. Aeronaut. Astronaut.*, 2009, 449. doi.org/10.2514/6.2009-449.

[48]. Tucker, P.K.; Menon, S.; Merkle, C.L.; Oefelein, J.C. & Yang, V. An approach to improved credibility of CFD simulations for rocket injector design. *Am. Inst. Aeronaut. Astronaut.*, 2007, 5572. doi.org/10.2514/6.2007-5572.

[49]. West, J.; Lin, J.; Tucker, K. & Chenoweth, J. Steady state combustion CFD analysis of local heat transfer for liquid oxygen/gaseous hydrogen injectors. 53rd JANNAF Propulsion Meeting/2nd Liquid Propulsion Subcommittee Meeting, December 5-8, Monterey, CA, USA, 2005.

[50]. Meinhardt, D.; Brewster, G.; Christofferson, S. & Wucherer, E. Development and testing of new, man-based monopropellants in small rocket thrusters. *Am. Inst. Aeronaut. Astronaut.*, 1998, 4006. doi.org/10.2514/6.1998-4006.

[51]. Smith, T.A.; Pavli, A.J. & Kacynski, K.J. Comparison of theoretical and experimental thrust performance of a 1030:1 area ratio rocket nozzle at a chamber pressure of 2413 kN/m^2 (350 psia). *Am. Inst. Aeronaut. Astronaut.*, 1987, 2069. doi.org/10.2514/6.1987-2069.

[52]. Sutton, G.P. & Biblarz, O. Rocket propulsion elements. John Wiley & Sons, Inc., New York, 2010.